

## FURTHER EVIDENCE FOR DIFFERENTIAL ROTATION IN V1057 CYGNI

ALAN D. WELTY, STEPHEN E. STROM,<sup>1</sup> AND KAREN M. STROM<sup>1</sup>

Five College Astronomy Department, University of Massachusetts

LEE W. HARTMANN<sup>1</sup> AND SCOTT J. KENYON<sup>1</sup>

Harvard-Smithsonian Center for Astrophysics

GARY L. GRASDALEN<sup>1</sup>

University of Wyoming

AND

JOHN R. STAUFFER<sup>1</sup>

NASA, Ames Research Center

Received 1989 April 10; accepted 1989 July 17

## ABSTRACT

Further tests of the accretion disk hypothesis for FU Orionis objects are presented. High spectral resolution, high signal to noise, 5820–6830 Å and 7500–9370 Å spectra of V1057 Cyg reveal a correlation between linewidth and line transition lower excitation potential expected from this hypothesis. The magnitude of the effect compares favorably with that predicted by synthetic disk spectra. Additional evidence for previously documented spectral type and linewidth versus wavelength correlations is also presented. This kinematic evidence strongly supports the accretion disk hypothesis.

*Subject headings:* stars: accretion — stars: individual (V1057 Cygni) — stars: pre-main-sequence

## I. INTRODUCTION

The FU Orionis objects have been the subject of much recent observational and theoretical study in the field of star formation. The most notable observational characteristic of the class is a 100 fold increase in luminosity, with a rise time of several months or years, followed by a slow decline over many decades. The best known and studied examples of the class are FU Ori and V1057 Cyg (LkHα 190). All known FU Ori objects are located within the boundaries of well-known star-forming complexes and display strong lithium absorption. Moreover, the only preoutburst spectrum of an FU Ori object, that of V1057 Cyg, is consistent with that of a T Tauri star (TTS) (Herbig 1977). Hence, it seems plausible that the precursors to the FU Ori objects are low-mass young stellar objects (YSOs); depending on  $\sin i$ ,  $M_* \sim 0.1 - 0.5 M_\odot$  is inferred directly for the central object in the V1057 Cyg system (Kenyon, Hartmann, and Hewett 1988, hereafter KHH).

Hartmann and Kenyon (1985, 1987a, b, KHH) propose that the rapid increase in luminosity for FU Ori objects results from a large increase in the accretion rate,  $\dot{M}$ , through a circumstellar disk; at maximum light the luminosity of an FU Ori object is, in this hypothesis, dominated by the accretion disk. Their model follows the formalism of Shakura and Sunyaev (1973) and Lynden-Bell and Pringle (1974) in attributing mass and angular momentum transport to viscous shear between adjacent disk annuli, producing radiant energy. The accretion luminosity,  $L_{\text{acc}}$ , is proportional to the mass accretion rate, and for the FU Ori objects,  $L_{\text{acc}} \gg L_*$  at all wavelengths,  $\lambda$ . The model assumes a steady accretion disk ( $\dot{M} = \text{constant}$ ), which implies  $T \propto R^{-3/4}$ , and an infrared spectral energy distribution with  $\lambda F_\lambda \propto \lambda^{-4/3}$ , consistent with the observed distributions for FU Ori objects. The accretion rates required by the model for FU

Ori and V1057 Cyg are  $M_* \dot{M} \sim (0.5-4) \times 10^{-4} M_\odot \text{ yr}^{-1}$  and  $(0.5-3) \times 10^{-4} M_\odot \text{ yr}^{-1}$ , respectively (KHH).

Hartmann and Kenyon also propose that the absorption line spectra of the FU Ori objects arise in the disk “photospheres,” whose “effective temperature” reflects the local disk temperature. If so, the temperature-radius relationship ( $T \propto R^{-3/4}$ ) should produce a variation of apparent spectral type with  $R$ . This effect should be observable as a variation of spectral type with wavelength: the optical spectrum is produced primarily in the hot inner portion of the disk, while the infrared spectrum is dominated by the higher surface area, cool outer regions of the disk. Two closely related effects should also be observable. Because disk material is assumed to be in Keplerian motion about the central object, the widths of absorption lines should reflect conditions in the regions of line formation. Specifically, linewidth is expected to (a) decrease with increasing wavelength, since line broadening is greatest in the more rapidly rotating inner disk and (b) increase with lower excitation potential,  $\chi$ , since high  $\chi$  levels are significantly populated only in the hot, inner disk.

Hartmann and Kenyon were able to predict the absorption line spectrum arising from the disk by assuming that the disk can be modeled as an ensemble of concentric annuli, each assumed to produce a spectrum identical to that of a star of spectral type corresponding to  $T(R)$ . The contribution from a given annulus is taken to be the spectrum of a standard star of a temperature fixed by the disk temperature-radius relation, scaled according to the emitting area of the annulus, and convolved with the broadening function appropriate to a rotating ring. The contributions from all annuli are added to produce the final “synthetic disk spectrum.” If the rotation velocity ( $v \sin i$ ) in the region of the disk contributing to the observed spectrum is large, significant doubling of line profiles will occur, due to the shape of the broadening function for lines formed in a rotating annulus.

The disk temperature-radius relation is determined from the

<sup>1</sup> Visiting Astronomer, Kitt Peak National Observatory, operated for the National Science Foundation by the Associated Universities for Research in Astronomy.

requirement that the broad-band spectral energy distribution of the disk fit the observations. Model disk spectra calculated in this way yield the expected effects and provide quantitative predictions for the linewidth versus wavelength and linewidth versus excitation potential relationships (see § III text and figures). Observation of these effects would constitute convincing *kinematic* evidence for the presence of circumstellar accretion disks in the FU Ori objects, and by inference from the preoutburst spectrum of V1057 Cyg, many of the T Tauri stars (TTS) as well.

Variation of spectral type with wavelength has been observed by several investigators (Herbig 1977; Mould *et al.* 1978; Shanin 1979; KHH). The first convincing evidence for differential rotation in a circumstellar disk (FU Ori) was provided by Hartmann and Kenyon (1987a), and for V1057 Cyg by Hartmann and Kenyon (1987b), by comparing optical and near-infrared rotational velocities. This paper offers further observational evidence for differential rotation, emphasizing its *continuous* nature, and reports the first observation of the increase of line width with increasing lower excitation potential.

## II. OBSERVATIONS AND DATA REDUCTION

To examine the linewidth versus lower excitation potential hypothesis, we require spectra with wavelength coverage sufficient to include a statistically significant number of usable absorption lines. If useful measurements of line width are to be obtained, several resolution elements must span each line. Optical absorption linewidths in FU Ori and V1057 Cyg are  $\sim 2 \text{ \AA}$  (Hartmann and Kenyon 1987a, b). Thus, echelle spectra of  $\sim 0.3 \text{ \AA}$  resolution and wavelength coverage of several hundred angstroms provide an ideal means of meeting these requirements.

We have used two sets of echelle spectra, spanning the 5820–7640  $\text{\AA}$  and 7500–9370  $\text{\AA}$  ranges. V1057 Cyg was observed on 1986 October 15 and December 15 with the 4 m Mayall telescope of the Kitt Peak National Observatory (KPNO). Spectra were obtained with the KPNO echelle and a Texas Instruments charge-coupled device (CCD). The UV fast camera with a 31.6 groove  $\text{mm}^{-1}$  echelle grating combined with a 226 groove  $\text{mm}^{-1}$  cross-disperser yields a dispersion of 8.3  $\text{\AA mm}^{-1}$  at 7500  $\text{\AA}$ , and 6.4  $\text{\AA mm}^{-1}$  at 5820  $\text{\AA}$ . Flat field exposures were taken to correct for pixel to pixel variations in CCD sensitivity. An LED was used to preflash each exposure, guaranteeing a background level sufficient to ensure linear CCD response at low light levels. Data was binned 2:1 perpendicular to the dispersion axis.

Initial processing was completed with KPNO's CCD reduction software. The flat field and bias exposures were combined into single flat field and bias images, respectively. The average bias image was subtracted from the raw V1057 Cyg image. This bias-subtracted image was then flat-fielded in the usual manner for echelle data.

Further reduction made use of KPNO's Image Reduction and Analysis Facility (IRAF), installed on the Five College Astronomy Department's VAX 11/750 and on the Harvard-Smithsonian Center for Astrophysics' Sun workstations. The intensity-wavelength vectors were extracted from the two-dimensional images. The 5820–7460  $\text{\AA}$  wavelength calibration was provided by the thorium-argon arc comparison spectrum. In the 7500–9370  $\text{\AA}$  region there are too few lines in our thorium-argon arc spectra to produce satisfactory wavelength calibration. Wavelength calibration of these data was

obtained by identifying absorption lines ( $\sim 8$ ) in each order of a standard star spectrum obtained the same night, determining the pixel-wavelength relationship, and applying the results to the V1057 Cyg orders. Typical rms deviations between actual wavelengths and fitted values are  $\sim 0.01 \text{ \AA}$  ( $\sim 0.35 \text{ km s}^{-1}$ ) or less. Definition of the rest velocity of the spectrograph system is provided by measuring the positions of telluric emission and absorption lines.

Spectra of standard stars were obtained with similar setups and reduction procedures. Standards used for comparison and modeling in the 7500–9370  $\text{\AA}$  region, observed 1986 October 14–15, are 70 Peg (G7 III),  $\epsilon$  Cyg (K0 III), 39 Cyg (K3 III),  $\alpha$  Tau (K5 III), and 24 Cap (M0.5 III). Observations indicate that V1057 Cyg is a low-gravity object (Herbig 1966) whose spectrum is best matched by supergiant standard star spectra (Hartmann and Kenyon 1987a, b, KHH). Unfortunately, because the 1986 October observing program was focused on observations of TTS, the standard stars observed were giants and dwarfs; no supergiant spectra were obtained. While strengths of model lines may thus be too weak, we note that any difference in line broadening between giants and supergiants, or between weak and strong lines, will be negligible compared to the broadening ( $\sim 35 \text{ km s}^{-1}$ ) characteristic of the V1057 Cyg lines. Thus, model linewidths will be acceptable.

We also observed standard stars in the 5120–6930  $\text{\AA}$  region for the purpose of modeling the V1057 Cyg spectrum. Specifically, spectra of SAO 22328 (F6 Ib), SAO 22740 (G2 Ib), SAO 22785 (K5 Ib), SAO 58528 (M1 II), and SAO 58322 (M2 Iab) were input to the disk model program. These standard stars and SAO 22593 (K2 II) were used for spectral type estimation. These data were obtained on 1988 January 4–5 at KPNO, using setups and reduction procedures similar to those of the 5820–7640  $\text{\AA}$  data described above, and have  $\sim 0.3 \text{ \AA}$  resolution. In the comparisons between stellar and model 6000  $\text{\AA}$  data which follow, we will discuss only the 5820–6930  $\text{\AA}$  overlap region, although the phenomena described are observed in the full ranges of both data sets.

## III. RESULTS AND DISCUSSION

Our first step was to identify all the strong ( $W_\lambda \gtrsim 100 \text{ m\AA}$ ) absorption lines in our V1057 Cyg spectra; stellar lines weaker than  $\sim 100 \text{ m\AA}$  generally cannot be seen at  $3\sigma$  confidence, owing to line broadening ( $\sim 35 \text{ km s}^{-1}$ ) and the finite signal-to-noise ratio of our data ( $\sim 100$  and  $\sim 140$  per pixel for the 7500–9370  $\text{\AA}$  and 5820–7640  $\text{\AA}$  data, respectively). Line identification was accomplished by comparing the V1057 Cyg spectrum with spectra of standard stars, solar spectrum line lists (Swenson *et al.* 1970; Moore, Minnaert, and Houtgast 1966), and the Revised Multiplet Table (Moore 1959). The region around each strong absorption feature was compared with the corresponding line in a standard star of comparable spectral type (see below) to remove blended lines from the list. Lines were deleted if another feature greater than  $\sim 10\%$  as strong occurred within the FWHM of the typical linewidth in V1057 Cyg ( $\sim 1.8 \text{ \AA}$ ).

High spectral resolution studies have demonstrated that line profiles in FU Ori, V1057 Cyg, and Z CMa are doubled, presumably due to line formation in a circumstellar disk (Hartmann and Kenyon 1987a, b; KHH; Hartmann *et al.* 1989). Therefore, having set the local continuum, visual examination of line profiles to determine half-intensity points is the appropriate method for estimating linewidths. Because profile doubling in V1057 Cyg is small, and profiles typically show

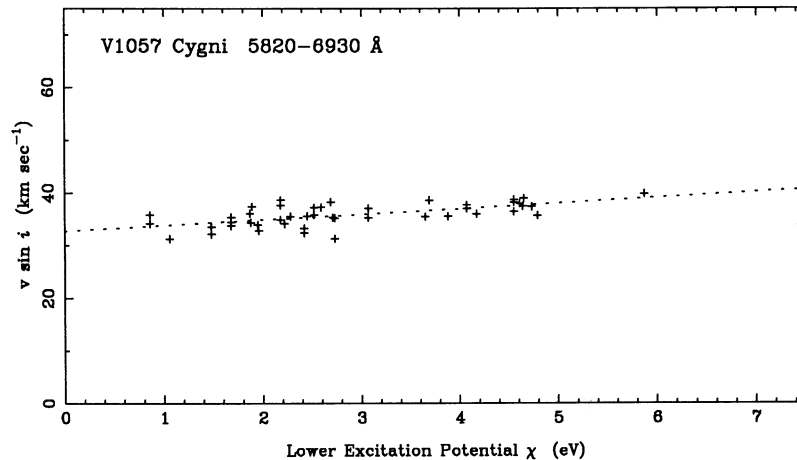


FIG. 1.—V1057 Cyg linewidths, converted to  $v \sin i$ , are plotted against lower excitation potential,  $\chi$ , for the wavelength range 5820–6930 Å. The slope is in the sense predicted (see text and Table 1), providing *kinematic* evidence for the presence of a circumstellar accretion disk in the V1057 Cyg system.

only subtle departures from symmetry, we also fit Gaussians to the lines to compare our “eye estimates” with more “objective” measurements. The Gaussian widths agree well with the eye estimation method: the rms deviation is  $\pm 3.2\%$  per point. In the discussion which follows, we have used the eye-estimated values.

If we are in fact observing disk “photospheres” of the FU Ori objects, we expect to observe a variation of *spectral type with wavelength*, as discussed in § I. While our spectral type estimates are *consistent* with previous spectral type determinations (see Kenyon and Hartmann 1988), our standard grids are not fine enough for us to make precise determinations for either wavelength range. Further, our 7500–9370 Å standards are giants (rather than supergiants), the earliest of which is G7, too late for us to bracket the spectral type in that range.

Our primary goal is to investigate the predicted relationship between linewidth and lower excitation potential. Figure 1 shows linewidth versus excitation potential for the optical (5820–6930 Å) data; Figure 2 is similar, but for the far red (7500–9370 Å) data. These figures provide evidence for the effect predicted, namely that the *higher excitation potential lines are broader* in our V1057 Cyg data. Table 1 contains a listing of slopes and intercepts for these figures and similar figures to be discussed below. These results may be considered

marginal ( $2.5\sigma$  for the optical and  $3.3\sigma$  for the far red), but the agreement with theory (see below) is encouraging. We will demonstrate that the result is not due to other correlations in our data, does not result from unknown bias in our measurement technique, asymmetries in line profiles, or blending, and that the scatter (rms deviation from fit  $\sim 2.5 \text{ km s}^{-1}$ ) is due largely to the finite signal to noise ratio of our data.

First, however, we note that Figures 1 and 2 also provide evidence of the *linewidth versus wavelength* relationship, discussed previously by Hartmann and Kenyon (1987a, b). We notice that the 5820–6930 Å lines tend to be broader than the 7500–9370 Å lines, as the intercepts for Figures 1 and 2 (see Table 1) demonstrate. We have used the *y*-intercept rather than the mean linewidth to measure this effect because the two line lists have significantly different distributions in  $\chi$  (cf. Figs. 1 and 2), which would weight the linewidth estimates incorrectly.

We have also plotted linewidth versus wavelength directly, in Figure 3, including lines in the 6930–7500 Å range. We have included only those lines in the 2–5 eV range because the lines of largest  $\chi$  tend to be the lines of longest wavelength. This is true in both wavelength ranges we observed. Inclusion of the high  $\chi$  lines, which tend to be broad, would thus tend to conceal the  $\Delta\lambda/\lambda$  versus  $\lambda$  relationship. We see in Figure 3 that linewidth seems to decrease continuously with wavelength

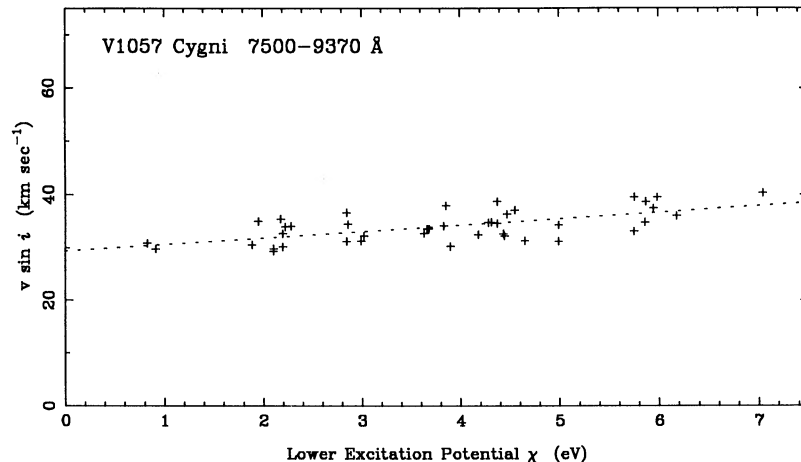


FIG. 2.—Same as Fig. 1, for the wavelength range 7500–9370 Å

TABLE 1  
 $v \sin i$  VERSUS  $\chi$  SLOPES AND INTERCEPTS

Figure	Data set	Slope (km s <sup>-1</sup> eV <sup>-1</sup> )	$\sigma_{\text{slope}}$ (km s <sup>-1</sup> eV <sup>-1</sup> )	Intercept (km s <sup>-1</sup> )	$\sigma_{\text{int}}$ (km s <sup>-1</sup> )	$n^a$	$r^b$
1.....	5820–6930 Å data	1.10	0.44	32.4	1.3	45	0.626
2.....	7500–9370 Å data	1.16	0.35	29.3	1.4	42	0.628
4.....	7500–9370 Å 70 Peg	-0.04	0.09	8.4	0.4	42	0.120
5.....	7500–9370 Å simulation	-0.19	0.35	33.6	1.4	42	0.108
6.....	5820–6930 Å model	1.19	0.43	31.3	1.3	45	0.566
7.....	7500–9370 Å model	1.26	0.35	28.7	1.4	42	0.714

<sup>a</sup>  $n$  is the number of lines in the data set.

<sup>b</sup>  $r$  is the linear correlation coefficient for the data.

over the observed wavelength range. The least-squares slope is  $-1.5 \pm 0.3$  km s<sup>-1</sup>/1000 Å. Similar analysis of model spectra (see below) yields the same slope, which corresponds roughly to the effect predicted by KHH.

#### a) Checks on the Result

To rule out the possibility that the observed linewidth versus excitation potential result is actually a reflection of another, more fundamental correlation, we plotted both  $\Delta\lambda/\lambda$  and  $\chi$  versus  $\lambda$ . As discussed, we expected and found a correlation between linewidth and wavelength (Fig. 3). We found no correlation between excitation potential and wavelength which might then lead to the  $\Delta\lambda/\lambda$  versus  $\chi$  result.

We performed the following crude simulation to rule out systematic error in our measurement procedure as an explanation for our result, and to investigate the origin of the scatter apparent in Figures 1 and 2. We measured the same lines in 70 Peg (G7) as in V1057 Cyg (in the 7500–9370 Å region); the results appear in Figure 4 and Table 1. Because lines in V1057 Cyg seem well approximated by Gaussians, we next artificially broadened the 70 Peg spectrum with a constant velocity-width Gaussian and added a spectrum of Gaussian-distributed, zero mean random numbers to reproduce (roughly) the line broadening and signal to noise in our V1057 Cyg data. Lines in the resulting spectrum were measured as for the real data; typical results of such tests appear in Figure 5 and Table 1. From this experiment we see that the scatter in measured linewidths for lines of similar lower excitation potential is consistent with origin in the finite signal to noise of our data.

Moreover, no runs of artificially noisy spectra yielded a significant  $\Delta\lambda/\lambda - \chi$  relationship.

Approximately 40% of the line profiles in V1057 Cyg appear to be noticeably asymmetric; the most common asymmetry ( $\sim 60\%$  of the 35 asymmetric lines in our list) is an enhanced blueward line wing. This is not predicted by the steady disk model, but might result from the contribution of a stellar wind component. We thus investigated the possible effect of a wind component on the measured linewidths. If such a component is significant, we expect a correlation between radial velocity,  $v_r$ , and  $\chi$ , since absorption components formed in the wind should be manifested more strongly in the lower  $\chi$  lines; because the wind is blueshifted relative to the disk, the low  $\chi$  lines should appear relatively more blueshifted than the high  $\chi$  lines. No correlation is observed, and the rms deviation from zero velocity (systemic) is 4.14 km s<sup>-1</sup>. We performed the same test for 70 Peg and a rotated, artificially noisy version of 70 Peg. No correlation is observed for either. The rms deviations, 1.15 km s<sup>-1</sup> and 4.95 km s<sup>-1</sup>, respectively, suggest that the apparent line asymmetries in our V1057 Cyg data are consistent with origin in the noise in our data (but see below).

Although effort was made to select isolated lines, some blending is undoubtedly present in the lines we used. Because weaker lines may be affected by blending more than strong lines, we investigated the possible effect of blending in the scatter in the previous test by plotting equivalent width,  $W_\lambda$ , versus radial velocity. There is no apparent correlation, and we conclude that blends are not a significant factor in affecting our results. We are left with the conclusion that our  $\Delta\lambda/\lambda$  versus  $\chi$

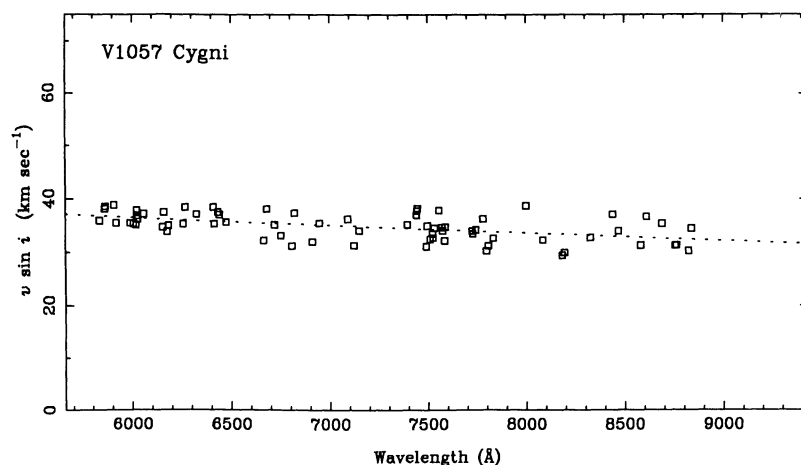


FIG. 3.—This plot of linewidth vs. wavelength for V1057 Cyg includes both data sets (5820–9370 Å, including the 6930–7500 Å range for which we have no corresponding model). Lines having lower excitation potential,  $\chi$ , less than 2 eV or greater than 5 eV have been excluded (see text).

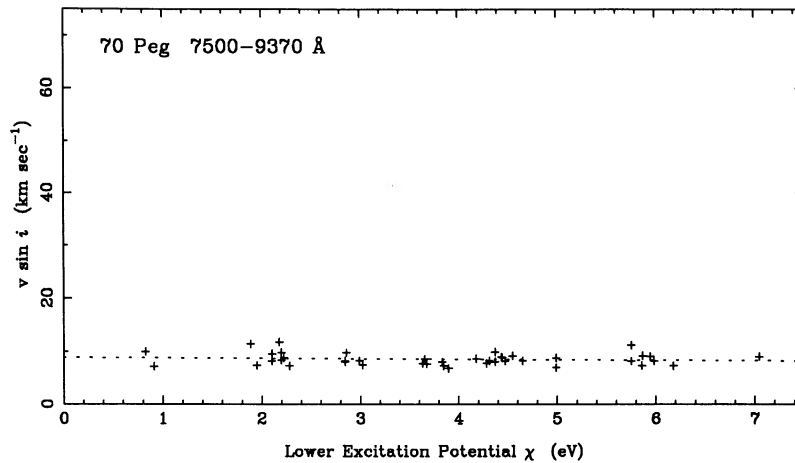


FIG. 4.—Same as Fig. 2, for 70 Peg (G7 III standard star). The small rotation velocity indicated is roughly the instrumental resolution.

result is best interpreted as a signature of the V1057 Cyg accretion disk.

#### b) Comparison with Theory

The spectrum of V1057 Cyg has been successfully modeled as a luminous accretion disk, as discussed in § I; more detail may be found in KHH. To make quantitative predictions for the linewidth versus excitation potential relationship, we have used the Hartmann-Kenyon model to obtain synthetic disk spectra for the 5820–6930 Å and 7500–9370 Å regions, using the standard star spectra listed in § II as input. We used the same method of analysis and same line list for the model spectra as for the V1057 Cyg data. Widths of lines in the model spectra are plotted as a function of  $\chi$  in Figures 6 and 7 for the 5820–6930 Å and 7500–9370 Å models, respectively. The slope in Figure 6 is  $1.19 \pm 0.43 \text{ km s}^{-1} \text{ eV}^{-1}$ , compared to  $1.10 \pm 0.44 \text{ km s}^{-1} \text{ eV}^{-1}$  for the corresponding stellar data in Figure 1, and the intercept is  $31.3 \pm 1.3 \text{ km s}^{-1}$  compared to  $32.4 \pm 1.3 \text{ km s}^{-1}$  in Figure 1. Agreement of slopes and intercepts are similarly good for the 7500–9370 Å stellar and model data in Figures 2 and 7 (see Table 1).

These model data also predict that linewidth decreases with wavelength. The intercept for the 5829–6930 model (Fig. 6) is  $31.3 \pm 1.3 \text{ km s}^{-1}$ , while the intercept for the 7500–9370 Å

model (Fig. 7) is  $28.7 \pm 1.4 \text{ km s}^{-1}$ , or 9.1% smaller. However, these results are significant at only  $1.6 \sigma$  and  $1.4 \sigma$ , respectively. Moreover, a plot of model linewidths versus wavelength (Fig. 8) yields a slope of  $-1.5 \pm 0.3 \text{ km s}^{-1}/1000 \text{ Å}$ , the same as for the V1057 Cyg data (Fig. 3).

Although we find no evidence in our V1057 Cyg data itself that a wind component to the absorption lines has significantly influenced our  $\Delta\lambda/\lambda$  versus  $\chi$  result, the sense of (the small) departure of the model predictions from the data is qualitatively consistent with a wind contribution: low  $\chi$  lines may be slightly broader in the real object than in the model, which does not attempt to include a wind.

Finally, we compare observed linewidths,  $v \sin i$ , with those predicted by the model directly in Figure 9. We conclude, from the unit slope ( $0.95 \pm 0.08$ ) and zero intercept ( $1.2 \pm 2.8 \text{ km s}^{-1}$ ) of the relationship that this relatively crude representation of the V1057 Cyg spectrum provides a very satisfactory fit to the observations.

#### IV. CONCLUSIONS

We have shown that the spectrum of V1057 Cyg is characterized by a relationship between absorption line width and lower excitation potential over the 5820–9370 Å range. Our observed relationship is in accord with theoretical modelling

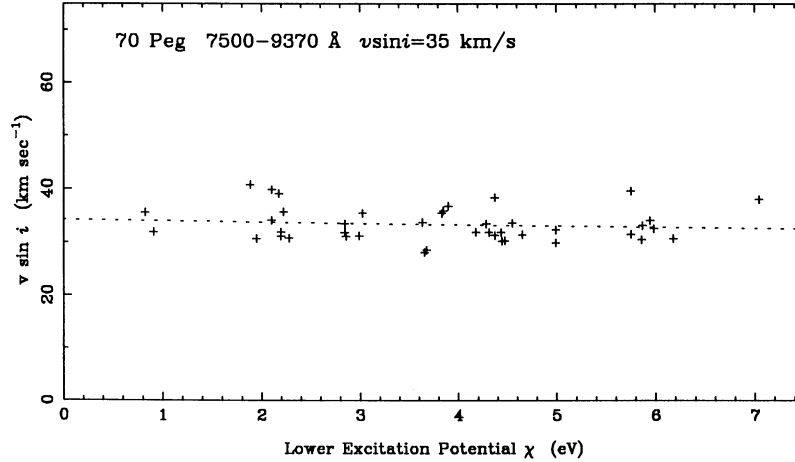


FIG. 5.—Same as Fig. 2, for 70 Peg (G7 III standard star) artificially broadened and noised to approximate the V1057 Cyg data. Because a single temperature is represented, no significant slope is expected.

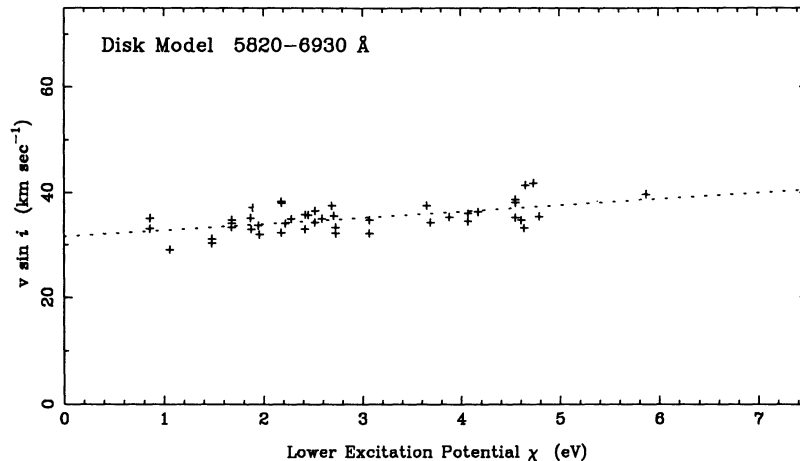


FIG. 6.—Same as Fig. 1, for the 5820–6930 Å model data

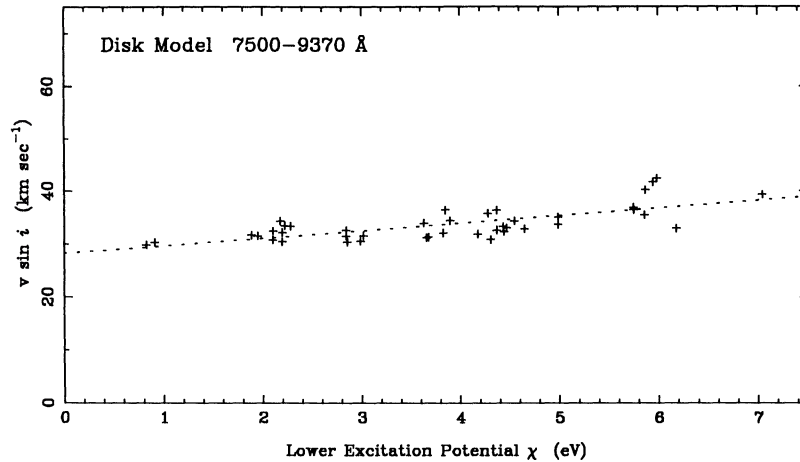
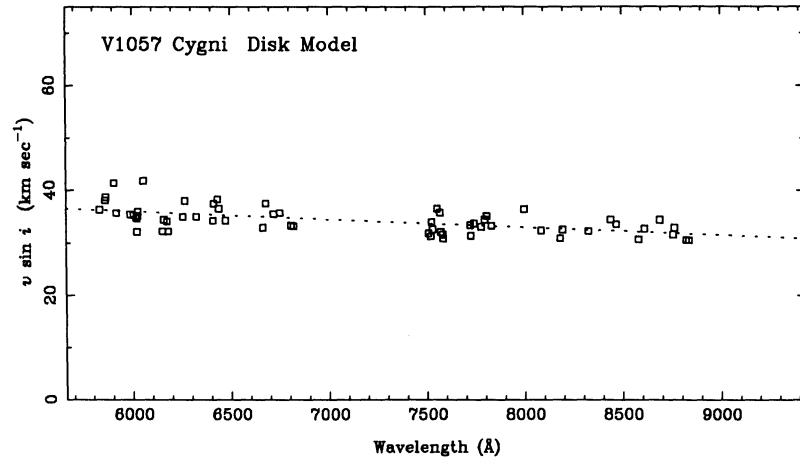


FIG. 7.—Same as Fig. 1, for the 7500–6397 Å model data

FIG. 8.—This plot of linewidth vs. wavelength for the V1057 Cyg model includes both data sets (5820–6930 Å and 7500–9300 Å). Lines having lower excitation potential,  $\chi$ , less than 2 eV or greater than 5 eV have been excluded (see text).

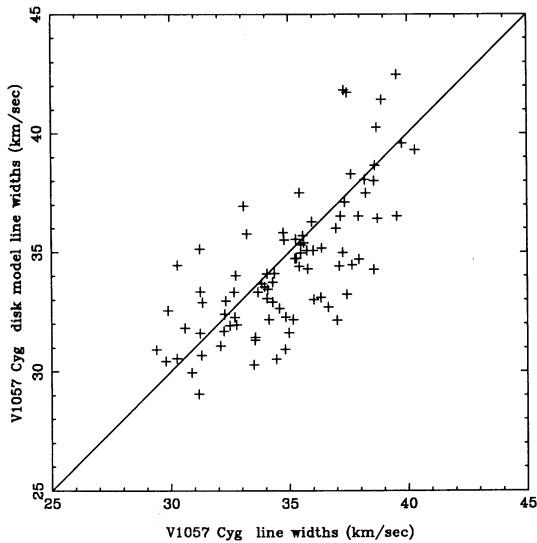


FIG. 9.—Comparison of linewidths ( $v \sin i$ ) in the V1057 Cyg spectrum and the corresponding lines in the disk model.

of V1057 Cyg as a self-luminous accretion disk, whose temperature-radius relationship is set only by the observed spectral energy distribution. We have also found evidence that absorption linewidth decreases continuously with wavelength, a relationship also predicted by theory. We conclude that the

observed line spectrum provides important kinematic evidence for the presence of a circumstellar accretion disk in the V1057 Cyg system.

The FU Ori objects not only possess luminous active accretion disks; they are also known to drive powerful winds (Croswell, Hartmann, and Avrett 1987). Comparison of stellar and synthetic model spectra hints that the wind emanating from V1057 Cyg may be affecting the observed absorption line spectrum in 5820–9370 Å region. This effect, if real, tends to mask, rather than enhance the linewidth versus excitation potential relationship. Hartmann and Kenyon (1987a; KHH) suggest that FU Ori winds are responsible for the blue-enhanced cross-correlation profiles in FU Ori and V1057 Cyg at 5200 Å as well. If so, an understanding of these winds and their effects is essential for a more complete understanding of the FU Ori phenomenon. With that goal in mind, we plan to explore the physics of FU Ori winds and disks further in a subsequent paper, using spectra of similar resolution, greater spectral coverage, and higher signal-to-noise than the present data.

We gratefully acknowledge the contribution of Robert Hewett, who constructed the disk model spectra presented here. A. D. W., S. E.S., and K. M.S. were supported by National Science Foundation and NASA Planetary Program grants. Portions of this research were also supported by the Scholarly Studies Program of the Smithsonian Institution.

#### REFERENCES

Croswell, K., Hartmann, L., and Avrett, E. H. 1987 *Ap. J.*, **312**, 227.  
 Hartmann, L. W., and Kenyon S. J. 1985, *Ap. J.*, **299**, 462.  
 —. 1987a, *Ap. J.*, **312**, 243.  
 —. 1987b, *Ap. J.*, **322**, 393.  
 Hartmann, L. W., Kenyon, S. J., Hewett, R., Edwards, S., Strom, K. M., Strom, S. E., and Stauffer, J. R. 1989 *Ap. J.*, **338**, 1001.  
 Herbig, G. 1966, *Vistas in Astronomy*, Vol. 8, ed. A. Beer and K. A. Strand (Oxford: Pergamon) p. 109.  
 —. 1977, *Ap. J.*, **223**, 213.  
 Kenyon, S. J., and Hartmann, L. W. 1988, *Pulsation and Mass Loss in Stars*, ed. R. Stalio and L. A. Willson (Dordrecht: Kluwer), p. 133.  
 Kenyon, S. J., Hartman, L. W., and Hewett, R. 1988, *Ap. J.*, **325**, 231 (KHH).  
 Lynden-Bell, D., and Pringle, J. E. 1974, *M.N.R.A.S.*, **168**, 603.  
 Moore, C. E. 1959, *A Multiplet Table of Astrophysical Interest* (TN 36, PB 151395, Department of Commerce, Clearing House for Federal and Scientific Information, Springfield, VA).  
 Moore, C. E., Minnaert, M. G. J., and Houtgast, J. 1966, *NBS Monog. 61, The Solar Spectrum 2935 Å to 8770 Å*, (Washington, DC: Department of Commerce).  
 Mould, J. R., Hall, D. N., Ridgway, S. T., Hintzen, P., and Aaronson, M. 1978, *Ap. J. (Letters)*, **222**, L123.  
 Shakura, N. I., and Sunyaev, R. A. 1973, *Astr. Ap.*, **24**, 337 (SS).  
 Shanin, G. I. 1979, *Astr. Zh.*, **56**, 288.  
 Swenson, J. W., Benedict, W. S., Delbouille, L., and Roland, G. 1970, *The Solar Spectrum from  $\lambda$ 7498 to  $\lambda$ 12016* (Liège: Société Royale des Sciences de Liège).

G. L. GRASDALEN: University Station, Box 3905, University of Wyoming, Laramie, WY 82071

L. W. HARTMANN and S. J. KENYON: Center for Astrophysics, 60 Garden Street, Cambridge, MA 02138

J. R. STAUFFER: NASA/Ames Research Center, MS 245-6, Moffett Field, CA 94035

K. M. STROM, S. E. STROM, and A. D. WELTY: Five College Astronomy Department, Lederle GRC 517G, University of Massachusetts, Amherst, MA 01003